Geochemistry, geothermometry and influence of the concentration of mobile elements in the chemical characteristics of carbonate-evaporitic thermal systems. The case of the Tiermas geothermal system (Spain)

M. Blasco[a,*], L.F. Auqué[a], M.J. Gimeno[a], P. Acero[a], M.P. Asta[b]

[a] Geochemical Modelling Group. Petrology and Geochemistry Area, Earth Sciences Department, University of Zaragoza, Spain C/ Pedro Cerbuna 12, 50009 Zaragoza, Spain.

[b] Environmental Microbiology Laboratory (EML), École Polytechnique Fédérale de Lausanne (EPFL). EPFL-ENAC-IIE-EML. Station 6, 1015, Lausanne, Switzerland.

[*] Corresponding author: Geochemical Modelling Group. Petrology and Geochemistry Area, Earth Sciences Department, University of Zaragoza, Spain. E-mail: monicabc@unizar.es; Tel.: +34 976761071; Fax: +34 976761106.

Abstract

The Tiermas low temperature geothermal system, hosted in the Paleocene-Eocene carbonates of the Jaca-Pamplona basin, has been studied to evaluate the geochemistry and the temperature of the waters in the deep reservoir. These waters are of chloride-sodium type and emerge with a temperature of about 37 ºC. Two hydrogeochemical groups of waters have been distinguished: one with lower sulphate concentration and lower TDS (about 7,500 ppm) and the other with higher sulphate content and TDS values (close to 11,000 ppm). There are also slight differences in the reservoir temperature estimated for each group. These temperatures have been determined by

combining several geothermometrical techniques: (1) classical chemical geothermometers (SiO_2-quartz, Na-K, K-Mg and Na-K-Ca), (2) specific geothermometers for carbonate systems (Ca-Mg), (3) isotopic geothermometers and, (4) geothermometrical modelling.

The good agreement in the temperature obtained by these techniques, including the cationic geothermometers which are not usually considered suitable for this type of systems, allows establishing a reliable range of temperature of 90 ± 20 ºC for the low-sulphate waters and 82 ± 15 ºC for the high-sulphate waters.

The mineral assemblage in equilibrium in the reservoir is assumed to be the same for both groups of waters (calcite, dolomite, quartz, anhydrite, albite, K-feldspar and other aluminosilicate phases); therefore, the differences found in the reservoir temperature and, mostly, in the geochemical characteristics of each group of waters must be due to the existence of two flow patterns, with slightly different temperatures and intensity of water-rock interaction.

Anhydrite is at equilibrium in the reservoir suggesting that, although this system is hosted in carbonates, evaporites may also be present. The dissolution of halite (the increase in the chloride concentration) conditions the chemical characteristics of the waters and the equilibrium situations in the reservoir and waters acquire their chloride-sodium affinity at depth and not during their ascent to the surface.

Finally, a favourable tectonic structure for CO_2 storage has been recognised in the Paleocene-Eocene carbonates of this area. Therefore, considering the characteristics of these waters (in equilibrium with calcite, dolomite and anhydrite in the reservoir), the results of this work are useful to understand some of the geochemical processes that might take place during the CO_2 injection: 1) precipitation of carbonates and sulphates

in the vicinity of the injection well due to desiccation of the waters and, 2) carbonate dissolution and sulphate precipitation in the long term.

Keywords: geothermal system; geothermometry; chemical geothermometers; isotopic geothermometers; geothermometrical modelling; mobile elements.

1. Introduction

Geothermal systems have always been of interest for industrial or touristic use of their waters (e.g., in greenhouses or balneotherapy). One of the first steps in the evaluation of the geothermal potential of an area is the study of the geochemical and isotopic characteristics of the thermal springs (e.g. D'Amore and Arnórsson, 2000). These studies provide information about the water evolution along the hydrological circuit and about its temperature in the reservoir. The general geochemical and geothermometric characterisation of the Tiermas geothermal system is presented in this paper.

The Tiermas thermal waters have been used in balneotherapy since Roman times. Nowadays the springs are covered by the waters impounded by the Yesa dam during most of the year. However, these springs become exposed frequently during late summer and many people come to benefit from their therapeutic properties. New projects to use these thermal waters again are being proposed. The spring temperature is about 40 ºC and the flow rate 200 L/s and they are considered one of the most important geothermal systems in Aragon for its geothermal potential (Sanchez, 2000; Sanchez *et al.*, 2004).

During the development of the ALGECO2 project, conducted by the Spanish Geological Survey (IGME), the Paleocene-Eocene carbonate rocks in this area (which is the most feasible aquifer of the Tiermas waters; see below) were considered a

favourable structure for CO_2 geological storage (Leyre-Berdún structure, southwards Leyre Sierra; Suárez *et al.*, 2014). This makes the study of these waters a potential analogue study for the ones expected to be in the proposed CO_2 storage, from which there are not yet hydrochemical data (Suárez et al, 2014; Gaus, 2010).

Despite the well known interest of the system, its hydrological and hydrochemical features are still poorly known due to the complex geology of the zone. Thus, the aim of this work is to fill in this gap with the geochemical characterisation of these waters and the estimation of the reservoir temperature using classical and geothermometrical modelling techniques.

2. Geological and hydrological setting

The Tiermas springs are located in the Aragonian pre-Pyrenees, in the northwest of the Zaragoza province (Figure 1). They emerge in the north shore of the Yesa reservoir, which covers the springs during most of the year. Geologically, the system is located in the Jaca-Pamplona Basin, between the Boltaña anticline and the Pamplona fault, and bounded on the north by the Axial Zone and the Inner Ranges and on the south by the Outer Ranges (Figure 2).The Jaca-Pamplona Basin is elongated in east-west direction, parallel to the general trend of the Pyrenees. Overall, the structure of the basin is an asymmetric syncline dipping south and filled with Tertiary formations (Larrasoaña *et al.*, 1996; Bauluz *et al.*, 2008). The evolution of this basin was conditioned by a compressional context. The South Pyrenean zone was a foreland basin during the Cretaceous and a deep trench opened westwards receiving sediments from a turbiditic system. In the Middle Eocene this basin was transformed in a piggy back basin, with southwards displacement due to the propagation of the South Pyrenean Basal Thrust and, eventually, was filled by tertiary sediments (Payros *et al.*, 1994; Oliva *et al.*, 1996).

The Jaca Basin has a great structural complexity: there are two main structural trends which give rise to two fault systems, one with a NNE-SSW direction, due to the reactivation of the tardi-hercynian fault systems, and the other with a E-W direction (Figure 1), that corresponds to the Pyreneean trend (IGME, 1973).

2.1. ***Stratigraphy***

Stratigraphically, the Jaca-Pamplona Basin is constituted by Triassic to Miocene formations with a sedimentary and metasedimentary Paleozoic basement (Saura and Teixell, 2006). The Triassic rocks belong to the Bundsandstein and Keuper Facies, with about 400 meters of conglomerates, sandstones and lutites, and 150 meters of evaporates, lutites and limestones , respectively (Pueyo *et al.*, 2012), although due to the role of the Keuper Facies as detachment level, it is difficult to determine its exact thickness. These Triassic formations are directly overlaid by a marine series deposited in the foreland South Pyreneean basin during the Upper Cretaceous: the Paleocene Alveoline Limestones, the Lower and Middle Eocene Guara Limestones and turbidites of the Hecho Group (IGME, 1973; Faci, 1997). This is followed by a regressive carbonate series in the Middle and Upper Eocene formed in an external platform and a prodelta system and constituted by the Sabiñanigo Sandstones (the Larres Marls in other areas), the Arguis-Pamplona marls and the Belsué-Atarés marls and sandstones. These formations are overlaid by evaporitic rocks, which indicate the transition to a paralic continental environment, and are constituted by halite, anhydrite and potassium salts (sylvite and carnalite) units (e.g. Ayora *et al.*, 1994, 1995). The potash units are restricted to the depocenter and they are mostly absent in the rest of locations (Ayora *et al.*, 1994); for instance, in the hydrocarbon exploration drilling Sangüesa 1 (Figure 1) these evaporites are only constituted by anhydrite and halite at depth.

Finally, the last stage of the basin evolution corresponds to the alluvial filling of the Jaca-Pamplona Basin that is represented in the Oligocene and Miocene continental formations (Campodarbe Group and Bernués and Uncastillo Formations; IGME, 1973; Faci, 1997).

In the context of this study, the Upper Cretaceous and the Paleocene-Eocene formations are of special interest as they constitute the potential geothermal formations (FG6 and FG7; Sánchez, 2000; Sánchez *et al.*, 2000, 2004) for the Tiermas thermal springs. The thickness of the Upper Cretaceous is about 200 metres in the area and it is constituted, at its base, by dolomitic limestones, marls and sandy limestones and, at the top, by the Marboré Sandstones (calcarenites with sandstones and siliceous conglomerates in the uppermost part; IGME, 1973; Faci, 1997).

In the Paleocene-Eocene formations, the Alveoline Limestones are 120 to 300 metres thick, and consist of carbonates and calcarenites, with sparitic or microsparitic cement, bioclasts, quartz grains and, locally, oncoids, ooids and intraclasts (IGME, 1973; Faci, 1997). The Guara Limestones in the area are about 100 metres thick and consist of bioclastic limestones with abundant siliciclastic rocks at the bottom that grade to marls towards the top (IGME, 1973; Puigdefâbregas, 1975; Faci, 1997). Exploratory drilling at depths between 2800 and 3700 metres show that these limestones from the Paleocene-Lower Eocene (Alveoline and Guara Limestones) are dolomitic at the bottom (Sánchez Guzmán and García de la Noceda, 2005). Finally, the Hecho Group consists of sets of siliciclastic turbidites and hemipelagic marls with calcite, illite, chlorite and minor albite and dolomite (Bauluz *et al.*, 2008). The most arenitic parts contain lithic fragments and clasts of quartz, plagioclase, K-feldspar and muscovite (Gupta and Pickering, 2008). Embedded in these materials appear the so-called carbonated mega-layers (or mega-turbidites), which are thick and laterally continuous carbonate-

cemented breccias and calcarenites, removed from a platform and re-deposited in a deep marine trench. Up to seven mega-layers with up to 200 meters of thickness have been identified in the Jaca-Pamplona Bain (IGME, 1973; Payros *et al.*, 1994; Faci, 1997; Bauluz *et al.*, 2008).

These formations, considered as the suitable aquifer of the waters studied here, although mainly constituted by carbonates, they also contain siliciclastic rocks, which will determine the geochemical characteristics of the waters (see below).

2.2. ***Hydrogeology***

Sánchez (2000) and Sánchez *et al.* (2000, 2004) distinguish several geothermal formations in the Pyrenees area defining them as "geological units able to store water or other fluids at a specific temperature and under specific mobility conditions suitable to allow some type of geothermal exploitation". Two of them, FG6 and FG7, are located in the studied area, the first one corresponds to the Upper Cretaceous formations and the second is formed by the Alveoline Limestones (Paleocene), the Guara Limestones (Paleocene-Eocene) and the megaturbidites from the Eocene Flysch. The second one is considered the potential aquifer of the Tiermas springs (ITGE-DGA, 1994; Faci, 1997; Sánchez, 2000; Sánchez *et al.*, 2000, 2004) and of the geothermal system of Jaca-Serrablo (about 70 km NE of Tiermas; Sánchez Guzmán and García de la Noceda, 2005).

The Tiermas waters are chloride-sodium/calcium-sulphate type with a TDS (total dissolved solids) higher than 10,000 ppm. Other waters also hosted in the Alveoline Limestones show different chemical features. For example, the groundwaters sampled in a piezometric borehole in Romanzado (12 km NW of Tiermas) are calcium-bicarbonate type (Consulnima, 2011) and the waters from the Jaca-Serrablo geothermal

system have TDS values around 2,000 ppm (Sánchez Guzmán and García de la Noceda, 2005). The lithological features of the potential aquifer of Tiermas springs (the Alveoline Limestones) do not include the presence of suitable rocks to provide a chloride-sodium/calcium-sulphate composition to the waters. One hypothesis is that the waters would acquire these chemical components during their ascent to surface due to the contact with the evaporites from the limit between the Upper Eocene and the Oligocene (ITGE-DGA, 1994). Another possibility could be that the structural complexity of the area (Figure 2) puts the waters in the deep reservoir into contact with the evaporitic rocks from the Keuper Facies or from the formations of the Eocene-Oligocene limit.

The possible areas proposed as recharge zones for the Tiermas geothermal system are outcrops of Paleocene and Eocene carbonates in the Leyre Sierra (Figure 1), in the Illon and Orba Sierras (Figure 1), and in the Inner Ranges (Figure 2; Auqué, 1993; ITGE-DGA, 1994; Sáenz, 1999; Consulnima, 2011). In any case, these springs result from the upward discharge of a deep (and, therefore, warm) groundwater flow. The rise of these waters to the surface is probably due to the NNE-SSE fractures that interrupt the N-S flow and force this to be vertical, resulting in a flow rate of about 200 L/s (Auqué, 1993; ITGE-DGA, 1994).

The limited information available about the Tiermas geothermal system and the structural complexity of the area makes the characterisation of the possible aquifer lithologies and the hydrological circuit, difficult.

3. Methodology

After reviewing the available analytical data about the Tiermas geothermal system, the unpublished results from the sampling campaign carried out in 1985 (Auqué, 1993)

were selected because this campaign produced a complete analytical data set including hydrochemical and isotopic data of the spring waters and *in situ* measurements of temperature, pH, and electrical conductivity. Another sample from 1991 (ITGE-DGA, 1994), taken in a shallow control borehole near the thermal springs, was included in this study to complete the characterisation of the system; in this case the electrical conductivity and pH were measured in the laboratory and there are no data for temperature, although an estimated value has been considered for this parameter. The rest of available chemical analyses since 1991 show a progressive decrease in the salinity of the thermal waters studied here. As they seem to represent a modification of the original situation in the thermal system (e.g. mixing and/or dilution) we decided to not consider them in this work. Table 1 compiles the chemical and physicochemical parameters for the selected samples indicating the laboratories where they were analysed.

The charge imbalance for the water samples was calculated with the PHREEQC code (Parkhurst and Appelo, 2013) and the results showed that all the samples have a charge imbalance lower than ± 5% (Table 1). This value is in the range usually accepted as valid (Nordstrom *et al.*, 1989; Appelo and Postma, 2005) and supports the reliability of the data used in this study. The lack of aluminium data in most of the samples has been solved by fixing the aluminium content in the water imposing equilibrium with an aluminosilicate phase in the geothermometrical modelling (Pang and Reed, 1998; Palandri and Reed, 2001).

3.1. ***Chemical and isotopic geothermometers***

The chemical geothermometers are the classical method to determine the reservoir temperature in geothermal systems. They use empiric or experimental calibrations based

on heterogeneous chemical reactions (temperature dependent) from which the equilibrium temperature can be calculated (e.g. Marini, 2004) using the elemental contents controlled by those heterogeneous reactions and assuming that the contents have not suffered significant changes during the rise of the waters to the surface.

A vast choice of geothermometers with various calibrations and suitable for different systems exists at present (e.g. see the review from D'Amore and Arnórsson, 2000). For example, the use of the cationic geothermometers (e.g. Na-K, K-Mg) has been proven very useful to estimate the reservoir temperature in high temperature systems (> 180 ºC), in which the equilibrium between the water and the minerals in the reservoir is generally reached. However, their use in intermediate to low temperature systems or in carbonate-evaporitic reservoirs, as the case studied here, is usually considered inappropriate due to the range of their calibration temperatures, the chemical features of the water used for the calibration and/or the mineral phases involved in the equilibrium situations (Auqué, 1993; Chiodini *et al.*, 1995; D'Amore and Arnórsson, 2000; Asta *et al.*, 2010). Despite these limitations, the K-Mg and silica geothermometers and some of their calibrations have been use here as they have provided good results in similar cases (Fernández *et al*., 1988*;* Michard and Bastide, 1988*;* Pastorelli *et al*., 1999; Wang *et al.* 2015). Moreover, as shown later, the use of the classical Giggenbach diagram (Giggenbach, 1988) indicates that Tiermas thermal waters fall on the field of the partially equilibrated waters, or near the fully equilibrate waters field, depending on the calibration considered, suggesting that the use of the cationic geothermometers, including the Na-K one, could be adequate.

The geothermometers that are more specific for low temperature carbonate-evaporitic systems and therefore more suitable for this study, are the Ca-Mg and the SO_4-F geothermometers, firstly developed by Marini *et al.* (1986) and then revised by Chiodini

240 *et al.* (1995). They are based on the assumption that Ca/Mg and SO_4/F ratios are mainly
241 controlled by temperature. The Ca-Mg geothermometer assumes the equilibrium of the
242 waters with calcite and dolomite in the reservoir, which is reasonable in this type of
243 systems. However, the results can be affected by the solubility of these mineral phases
244 and whilst the calcite solubility is quite well known, the solubility of the dolomite
245 depends on the degree of order/disorder. With respect to the SO_4-F geothermometer, it
246 can only be applied to waters fully equilibrated with anhydrite and fluorite in the
247 reservoir (Chiodini *et al*., 1995), which is not always the case in this type of systems.
248 The chemical geothermometers and calibrations finally selected are listed in Table 2.

249 Additionally, various isotopic geothermometers have been used including $\delta^{13}C$ CO_2-
250 HCO_3, $\delta^{18}O$ CO_2-H_2O and $\delta^{18}O$ SO_4-H_2O (Table 3). These geothermometers are based
251 on the assumption that two species are in isotopic equilibrium and the isotope exchange
252 is a function of temperature. These geothermometers could also present problems
253 associated to reequilibrium processes during the ascent of the waters and to the
254 calibrations. In order to take this into consideration, several calibrations have been used
255 for the geothermometer $\delta^{18}O$ in SO_4-H_2O (Boschetti, 2013): the classical calibrations
256 based in the HSO_4-H_2O exchange (Friedman and O'Neil, 1977; Seal *et al.*, 2000), and
257 the more recent ones based on the SO_4^{2-}-H_2O (Halas and Pluta, 2000; Zeebe, 2010) and
258 $CaSO_4$-H_2O exchange (Boschetti *et al.*, 2011).

259 ### 3.2. ***Geothermometrical modelling***

260 This modelling is based on the same assumption as the classical chemical
261 geothermometers: the thermal waters have reached the equilibrium with respect to the
262 minerals in contact with them in the reservoir of the geothermal system. Then, during
263 the ascent to the surface, the waters cool and change the distribution of the dissolved

species and, therefore, their saturation states with respect to the various minerals. The modelling consists in reverse the ascent of the waters simulating a progressive increase of the temperature up to a range in which the saturation states of the waters with respect to several minerals (presumably present in the reservoir) coincide in an equilibrium situation.

This technique was initially proposed for its use in alkaline thermal waters by Michard and his co-workers (Michard and Fouillac, 1980; Michard and Roekens, 1983; Michard *et al.*, 1986) and later generalised for other types of thermal systems by Reed and co-workers (Reed and Spycher, 1984; Pang and Reed, 1998; Palandri and Reed, 2001; Peiffer *et al.*, 2014; Spycher *et al.*, 2014). It presents some advantages over the chemical geothermometers: a) it gives a better identification of the mineral set in equilibrium with waters and of the chemical characteristics of the thermal waters at depths (pH, for instance); and b) it allows identifying the action and effects of secondary processes during the ascent of the thermal waters to surface such as mineral reequilibria, mixing with colder waters or outgassing processes (Michard and Fouillac, 1980; Michard and Roekens, 1983; Reed and Spycher, 1984; Michard *et al.*, 1986; Tole *et al.*, 1993; Pang and Reed, 1998; Palandri and Reed, 2001).

In this study PHREEQC code (Parkhurst and Appelo, 2013) has been used to carry out the geothermometrical modelling, using the LLNL thermodynamic database distributed with the code.

4. Results

4.1. *Chemical characteristics of the waters*

The water samples studied here were taken from four springs in 1985 (T1, T2, T3 and T4; Table 1) and from a shallow borehole in 1991 (B1; Table 1), all of them located in an area of 50 m^2. These samples are separated into two groups: low-sulphate samples, B1 and T1, with low sulphate concentration and low TDS (about 7,500 ppm; Table 1) and high-sulphate samples, T2, T3 and T4, with higher sulphate contents and higher TDS values (close to 11,000 ppm; Table 1). These two groups also present differences and similarities in some molar ratios:

- The Na/Cl ratio is near 1 for the samples of the low-sulphate group and higher for the samples of the high-sulphate one (approximately 1.6). This indicates that the Na and Cl concentrations in the low-sulphate group are controlled mainly by halite dissolution. Whereas, the 1.6 value in the high-sulphate group indicates an extra contribution of Na (e.g. associated to cation exchange).
- The Ca/SO_4 ratio in the low-sulphate group is about 0.6, and 0.2 in the high-sulphate. In both cases, as the contents of SO_4 are assumed to be controlled, almost entirely, by anhydrite dissolution, calcium must be removed from the waters by precipitation of other minerals, probably carbonates, or by cation exchange reactions.
- The Ca/HCO_3 and $Ca+Mg/HCO_3$ ratios are quite similar in both groups (about 2 and 3, respectively), although both are a little higher in the high-sulphate group. These ratios, much higher than 1, would reflect the important contribution of anhydrite dissolution in these waters.
- The $Ca+Mg/HCO_3+SO_4$ ratio (in eq/L) ranges between 0.85 and 0.88 (~ 1) in both groups. This indicates an important participation of interaction processes involving carbonates and sulphates, but with some additional intervention of other water-rock interaction processes.

- The K/Cl ratio is much lower than 1 in both groups (about 0.01) which means that sylvite is not a mineral phase with significant influence in the chemical characteristics of the waters. The same can be said about carnalite since the relation Cl:Mg:K in this phase is 3:1:1 and in the thermal waters is completely different (around 100:4:1). These facts suggest that the waters are not in contact with the evaporitic Eocene-Oligocene or that these rocks do not contain these minerals.
- Finally, the Mg/Ca ratio has similar values in both groups, ranging between 0.42 and 0.55, which could be indicative of a calcite-dolomite equilibrium at similar salinities and temperatures in the reservoir.

These ratios show that the chemical characteristics of both water types are highly influenced by carbonate and sulphate phases. Despite the similar spring temperature in both groups, the differences found in the chemical characteristics could be indicative of the existence of two flow patterns affected by different intensities of water-rock interaction processes.

For the two low-sulphate samples, B1 and T1, (Table 1) the lower concentration of sulphate in T1 could result from sulphate reduction despite the fact that there is not a significant increase in the HCO_3^- concentration compared to B1. The Tiermas thermal waters usually present a rotten eggs smell and have been described as sulfidic (e.g. Jimenez, 1838); therefore, the influence of sulphate reduction is feasible. A removal of the HCO_3^- upon sulphate reduction results from the precipitation of a carbonate phase, which would also explain the lower content of calcium in sample T1).

4.2. *Isotopic characteristics of the waters*

The isotopic data used here correspond to two samples from 1985: sample T1 and a sample from the Yesa reservoir (Table 4). The $\delta^{18}O$-$\delta^{2}H$ isotopic ratio for these waters (and other unpublished data from the Yesa reservoir in 2012 and one sample from a borehole in Tiermas; Baeza *et al.*, 2000; Figure 3) is close to the Global Meteoric Water Line $\delta^{2}H = 8 \cdot \delta^{18}O + 10$, defined by Craig (1961), the Regional Meteoric Water Line for Spain $\delta^{2}H = 8 \cdot \delta^{18}O + 9.27$ (Díaz-Teijeiro *et al.*, 2009) and also to the Local Meteoric Water Line, $\delta^{2}H = 5.6 \cdot \delta^{18}O - 7.6$ (Baeza *et al.*, 2000), which supports a meteoric origin for these waters (Figure 3). In high-temperature thermal systems, a positive $\delta^{18}O$-shift is observed (e.g. Clark and Fritz, 1997) and since the Tiermas thermal waters do not display such enrichment, this system should be regarded as low-medium temperature.

$\delta^{18}O$ and $\delta^{2}H$ in meteoric waters are negatively correlated with altitude (e.g. Clark and Fritz, 1997) and therefore, the depleted values for ^{18}O and ^{2}H in the thermal water indicate a higher elevation for its recharge area than for that of the waters in the Yesa reservoir. Unfortunately, there are no available regional data of the isotopic gradient with altitude which would have allowed determining the recharge area more accurately.

Finally, tritium in the thermal waters is below detection limit (Table 4) indicating a recharge prior to 1952 and that they are not affected by mixing with more recent waters (Clark and Fritz, 1997).

Some complementary information exists about the isotopic composition of the sulphates in the evaporites that might be in contact with these thermal waters. The Keuper Facies presents values of 10.9-16.3 ‰ for the $\delta^{34}S$ and 8.9-14.9 ‰ for $\delta^{18}O$ (Utrilla *et al.*, 1987). The isotopic values in the rocks of the limit between the Upper Eocene and the Oligocene are in the range of 12.9-23.6 ‰ for the $\delta^{34}S$ and 9.8-11.9 ‰ for $\delta^{18}O$ (Ayora *et al.*, 1995). The isotopic values in the dissolved sulphate of the thermal waters are

within these ranges, except that the $\delta^{34}S$ in the dissolved sulphate is slightly higher than the range reported for the Keuper facies (which could be explained by the sulphate reduction process that affects sample T1). In any case, these data support the hypothesis that the waters are in contact with some of these evaporites although, with the available data and considering the structural complexity of the area, it is not so clear if they are in contact with the Keuper Facies or with the evaporitic rocks of Upper Eocene-Oligocene limit.

4.3. *Saturation states*

The results obtained from the speciation-solubility calculations at spring temperature are shown in Table 5. Except for sample B1 that is oversaturated, the waters are close to equilibrium or slightly undersaturated with respect to calcite, and more undersaturated with respect to disordered dolomite. Their pCO_2 values are higher than the atmosphere and the oversaturation shown by sample B1 (related with its lower pCO_2) is possibly a result of CO_2 degassing before the pH was measured in laboratory. Waters are almost in equilibrium with chalcedony and are oversaturated with respect to quartz. They are undersaturated with respect to gypsum, anhydrite, fluorite, and also with respect to other evaporitic phases like halite, sylvite and carnalite. T1 is the only sample with aluminium concentration and it is clearly oversaturated with respect to albite, K-feldspar, and other aluminosilicates potentially present in the reservoir such as kaolinite, phyrophyllite, laumontite or clinochlore.

4.4. *Geothermometrical calculations*

4.4.1. Chemical geothermometers

The temperatures calculated (Table 6) with all the silica geothermometers are similar for all samples because their silica contents are also similar. The SiO_2-quartz geothermometer yields 75-78 °C (B1 is near 70 ºC because its silica content is lower than the rest) whilst the SiO_2-chalcedony geothermometer yields lower temperatures, 44-48 ºC (38 ºC for B1).

The K-Mg geothermometer provides values between 66 and 75 °C for all the samples, closer to those deduced with the SiO_2-quartz geothermometer. The results obtained with the other cationic geothermometers show substantial differences depending on the sample considered and in the case of the Na-K geothermometer the temperature predicted also depends on the calibration considered: 1) for the samples of the low-sulphate group (B1 and T1), the temperature is about 120 ºC with the Giggenbach (1988) calibration and about 100 ºC with the Fournier (1979) one; 2) for the samples of the high-sulphate group, the temperatures are around 95 and 75 ºC with the two calibrations, respectively. Given the good agreement between the result obtained with the K-Mg geothermometer and the Fournier (1979) Na-K calibration for the samples from the high-sulphate group (which is coherent with their position closer to the fully equilibrated waters in the Giggenbach diagram, Figure 4), only the Fournier calibration is considered in the discussions.

Finally, with respect to the rest of the cationic geothermometers: 1) the Na-K-Ca geothermometer (with $\beta = 1/3$ as recommended by Fournier and Truesdell, 1973) predicts a temperature close to 100 ºC for the samples of the high-sulphate group and slightly higher for the low-sulphate waters; 2) the Ca-Mg geothermometer predicts a temperature in the range between 75 and 88 ºC, consistent with the similar Mg/Ca ratios and salinities for all the samples; and 3) the SO_4-F geothermometer provides incoherent results in this case as fluorite has not reached the equilibrium in the reservoir.

As a general trend, the temperatures obtained with most of the chemical geothermometers are more similar to the ones deduced with the quartz geothermometer than to those provided by the chalcedony geothermometer, suggesting that quartz is the phase that probably controls the dissolved silica in the thermal waters of Tiermas.

Despite the slight differences provided by some geothermometers, the temperature values in the two groups of waters are quite similar and a temperature range of 85 ± 17 °C could be proposed for both. This range would include nearly all temperature values obtained (Table 6) and it is acceptable as it is similar to the uncertainty range for these determinations (± 20 °C; Fournier, 1982). Moreover, the 85 ºC range is indicated by the Ca-Mg geothermometer, which is specific for low temperature carbonate-evaporite systems and also by various cationic geothermometers with different sensitivity to secondary processes during the water ascent (D' Amore *et al*., 1987; D' Amore and Arnòrsson, 2000), suggesting that secondary effects are negligible.

4.4.2. Isotopic geothermometers

The results of the isotopic geothermometers calculations for sample T1 (from the low-sulphate group; Table 4) are shown in Table 7.

The $\delta^{13}C$ CO_2-HCO_3 geothermometer points towards different temperature values depending on the considered calibration. The Mook *et al.* (1974) calibration predicts a temperature of 70 ºC while with the Deines *et al.* (1974) it is 91 ºC. If the $\delta^{18}O$ CO_2-H_2O geothermometer is considered, the temperature predicted by various calibrations is quite similar, between 94 and 98 ºC (Table 7).

With respect to the $\delta^{18}O$ SO_4-H_2O geothermometer, using the classical calibrations (based on the equilibrium exchange between HSO_4^- and H_2O) the temperature ranges from 71 to 75 ºC whilst with the recently proposed calibrations based on the equilibrium

exchange between SO_4^{2-} and H_2O (Halas and Pluta, 2000; Zeebe, 2010), the temperatures obtained are very low (Table 7). Finally, using the calibration proposed in Boschetti *et al.* (2011; a combination of the calibrations of Chiba *et al.*, 1981 and Zheng, 1999), based on the equilibrium exchange between anhydrite ($CaSO_4$) and H_2O, the calculated temperature is 81 ºC.

The results of the calibrations based on the exchange between waters and various sulphur species, depend on the dominant species in solution (Boschetti, 2013). In low temperature systems with pH close to neutral, as in the Tiermas waters, SO_4^{2-} is usually the dominant species (70 % of the sulphate, in speciation calculations), nonetheless, these calibrations provide unreasonably low temperatures. This fact is probably due to the lack of equilibrium between SO_4^{2-} and H_2O since, in low temperature systems, the ^{18}O exchange between SO_4^{2-} and H_2O is slow and, moreover, the equilibrium can be affected by the sulphate reduction process identified in this sample (Boschetti *et al.*, 2011).

The calibration based on $\delta^{18}O$ $CaSO_4$-H_2O may be the most reliable for this system as it provides a temperature of 81 ºC quite similar to the results obtained from the previous calculations. Moreover, as it will be seen with the geothermometrical modelling next, the waters in the reservoir are in equilibrium with anhydrite.

The calibrations based on the $\delta^{18}O$ HSO_4^--H_2O exchange also provide reasonable temperatures despite the fact that they are suitable for acidic waters. This is due to the fact that these calibrations have almost the same position in the $\delta^{18}O$-T plot, as the one based on the $CaSO_4$-H_2O exchange for neutral water (see, for instance, Boschetti, 2013 or Awaleh *et al.*, 2015).

In summary, the values obtained by the isotopic geothermometers are in good agreement with those calculated with the chemical geothermometers.

4.4.3. Geothermometrical modelling

The geothermometrical modelling consists of simulating a progressive increase of water temperature to obtain the value for which a set of minerals, assumed to be present in the reservoir in equilibrium with the waters, simultaneously reach that equilibrium. The selection of the mineral phases is based on the hydrogeochemical characteristics of the studied waters, the reservoir lithology and the results obtained from the chemical geothermometers.

The evolution of these waters is assumed to be controlled by the interaction processes with carbonate and evaporitic rocks. Therefore, phases such as calcite, dolomite and anhydrite are included in the calculations. Other evaporitic minerals, such as halite, may have influenced the water composition but they were not included in the modelling because all the waters are strongly undersaturated with respect to them (Table 5).

The presence of detrital material in the carbonate aquifer diversifies the mineral set to consider. Minerals such as albite, K-feldspar and quartz have been identified in some of these formations and the success of the Na-K geothermometers (based on the existence of a K-feldspar-albite-solution equilibrium) and SiO_2-quartz (based on the existence of a quartz-solution equilibrium) supports that these phases could control some compositional characteristics of the waters.

Other aluminosilicate phases such as smectite, illite, chlorite and kaolinite are common in all types of sedimentary lithologies. Nevertheless, the solubility of such phases presents remarkable uncertainties due to their variability in composition, degree of crystallinity, etc. (Merino and Ransom, 1982; Nordstrom *et al.*, 1990; Palandri and

476 Reed, 2001). After testing various aluminium phases, clinochlore was chosen in this
477 study as representative for them, since it provides coherent results.

478 Some differences were found in the results obtained for the two samples of the low-
479 sulphate group (B1 and T1) and they are shown separately in Figure 5. The modelling
480 results for the samples from the high-sulphate group are, however, all similar and only
481 T3 is shown as representative in Figure 6.

482 The first results obtained for all the waters showed that calcite and dolomite reach
483 equilibrium at temperatures about 50 to 60 ºC, lower that the temperatures for the rest of
484 the considered mineral phases. Assuming that these minerals should be in equilibrium in
485 the reservoir in this type of systems, the lack of coincidence with the rest of the minerals
486 in equilibrium could be explained by CO_2 outgassing during the ascent of the waters to
487 the surface, which is coherent with the high pCO_2 values in the waters (Table 5). In
488 order to reconstruct the most plausible characteristics of the waters in the reservoir, and
489 to check this hypothesis, an increase of the CO_2 was simulated (as recommended by
490 Pang and Reed, 1998 or Palandri and Reed, 2001) to obtain an equilibrium temperature
491 for calcite similar to the temperature for the rest of phases. Although dolomite presents
492 more uncertainties than calcite, after adjusting the calcite equilibrium, dolomite also
493 provides coherent results.

494 The CO_2 in B1 was increased to about 9.6 mmol/L, which means a pH = 6 in the
495 reservoir, in sample T1 the increase was to 7.5 mmol/L and the pH was 6.15 and,
496 finally, the increase in sample T3 was to about 5.4 mmol/L, which yields pH = 6.45 at
497 depth. The results presented below in Table 8 and Figures 5 and 6 were obtained after
498 this reconstruction.

The results for sample T1 (Figure 5a and Table 8) show that the aluminosilicate phases (clinochlore, K-feldspar and albite) reach equilibrium at a temperature around 95 ºC, similar to the temperature predicted by dolomite (100 ºC). The temperature predicted by quartz is 72 ºC and by anhydrite is the highest, 113 ºC. Sample B1, with no aluminium data and with silica concentration lower than expected compared to the rest of samples, has been equilibrated with quartz and K-feldspar, as proposed by Palandri and Reed (2001), fixing the dissolved silica and aluminium contents. The results obtained for the rest of the minerals are about 100 ºC, (Figure 5b and Table 8). Even anhydrite reaches equilibrium in the same range as the other minerals since the sulphate content in this sample is higher than in sample T1.

The evolution with the temperature of the saturation indices of the selected minerals for sample T3 (representative of the high-sulphate group) is shown in Figure 6. Since there is not aluminium data for this sample, its concentration was fixed by imposing the K-feldspar equilibrium (Pang and Reed, 1998; Palandri and Reed, 2001). The results show a remarkable degree of convergence for the saturation indices of quartz and anhydrite which reach equilibrium at the same temperature, 72 and 71 ºC, respectively. These phases are highly reliable in geothermometrical determinations (Kharaka and Mariner, 1989; Auqué, 1993; Pastorelli *et al.* 1999), since they are thermodynamically well characterised and their saturation states are not affected by pH variations during the ascent of thermal waters. On top of that, they are independent of uncertainties from the aluminium concentration of the waters. With respect to the rest of the minerals, albite provides a temperature of 81 ºC whilst clinochlore and dolomite slightly higher (probably because these last two minerals can still be affected by some uncertainties due to the order degree in the first case, and the variations in its composition and crystallinity in the second; Helgeson et al, 1978; Palandri and Reed, 2001).

In summary, the temperature range deduced for the samples in the low-sulphate group is 101 ± 6 ºC and 92 ± 20 ºC for B1 and T1, respectively, and the temperature range predicted for sample T3 (as representative of the high-sulphate group) is somewhat lower, 84 ± 13 ºC.

5. Discussion

Combining the results obtained with the various geothermometrical techniques, the temperature in the reservoir deduced from each group is slightly different.

Temperature in the low sulphate group is higher, about 90 ºC, and although the results show a more widespread temperature range than for the high-sulphate group, they are in a reasonable uncertainty range (± 20 ºC; Fournier, 1982 and Tole *et al.*, 1993). The SiO_2-quartz and K-Mg geothermometers predict slightly lower temperatures for sample B1 (68 and 66 ºC, respectively), which could be due to secondary processes (e.g. dissolution/precipitation) affecting silica and magnesium contents (D'Amore and Arnórsson, 2000). Anhydrite provides a high temperature (113 ºC) for sample T1 (with lower sulphate content probably due to sulphate reduction), whilst for sample B1 (with higher sulphate content), anhydrite reaches equilibrium also close to 90 ºC. Therefore, if the temperature indicated by anhydrite in sample T1 is not considered representative of the conditions at depth, the temperature range defined for the waters of the low sulphate group in the reservoir would be 90 ± 20 ºC.

The good agreement of the results obtained with chemical geothermometers and geochemical modelling for the waters of the high-sulphate group suggests that the effects of secondary processes are not important and a lower temperature in the reservoir is indicated, 82 ± 15 ºC.

A remarkable finding is that equilibrium with albite and K-feldspar in the reservoir is evidenced with the geothermometrical modelling and the chemical geothermometers. This is not a common situation in low temperature carbonate-evaporitic systems. This equilibrium has been identified in some other "complex" carbonate-evaporitic system in which waters were also in contact with metasedimentary rocks (Marini *et al.*, 2000), whilst other authors reported equilibrium with respect to albite but not with respect to K-feldspar in similar geothermal systems (e.g. López-Chicano *et al.*, 2001; Boschetti *et al.*, 2005). The possible explanation for this equilibrium in a carbonate-evaporitic systems is that the aquifer formations contain a significant amount of detrital material, as indicated by López Chicano *et al.* (2001), allowing the waters to reach the equilibrium with phases like albite, K-feldspar and other aluminosilicate phases, as also evidenced here in the geothermometrical modelling.

Despite the compositional differences, the waters of both groups seem to have reached the equilibrium with the same mineral assemblage in the reservoir (calcite, dolomite, quartz, anhydrite, albite, K-feldspar and other aluminosilicate phases) and at quite similar temperatures. Therefore the compositional differences between the groups must be due to different extent of reaction with the evaporitic minerals and/or to the participation of additional reactions along the flow paths (as reflected in the Na/Cl and Ca/SO_4 ratios).

One of the main conclusions is that the equilibrium of these thermal waters with respect to anhydrite in the reservoir implies they must acquire the chloride-sodium/calcium-sulphate composition at depth and not while ascending to surface, otherwise, this equilibrium would not exist. However, with the available data, it is not possible to certainly determine if the evaporitic rocks in contact with the waters in the reservoir are those of the Keuper facies or those of the Eocene-Oligocene limit.

572 Although the degree of knowledge of this system is not enough to quantify the different
573 intensity in the water-rock interaction processes, two relevant issues can be discussed
574 from these results: 1) the influence of halite dissolution in the chemical characteristics
575 of the waters; and 2) the implications that the chemical character of these waters could
576 have for CO_2 storage in the reservoir formations.

577 ### 5.1. *The influence of halite dissolution in the chemical characteristics of the*
578 *waters*

579 The chemical characteristics of a water in equilibrium with a set of minerals are
580 conditioned by the temperature and the pressure at which this equilibrium is attained;
581 but they also depend on the concentration of elements not controlled by mineral
582 equilibria such as chloride or sulphate, the mobile elements of Michard (1987). The
583 influence of mobile elements, especially chloride, was recognised long ago by Helgeson
584 (1970) and chloride has been considered as an independent master variable in
585 determining the water composition in rock-buffered systems (Hanor, 2001). This
586 importance has been verified in various types of geothermal systems (Michard, 1987;
587 Michard and Bastide, 1988; Michard *et* al, 1996; Chiodini *et al.*, 1991), in low
588 temperature groundwaters in crystalline systems (Grimaud *et al* 1990; Trotignon *et al*,
589 1999) and in saline waters in sedimentary basins (Hanor, 1994; 1996; 2001).

590 The influence of the mobile elements are especially important in carbonate-evaporitic
591 geothermal systems because the waters are likely to be in contact with halite and its
592 dissolution will condition the chemistry of the waters in equilibrium with a specific
593 mineral set. This influence has been tested in the Tiermas thermal waters using the
594 reaction-path capabilities of PHREEQC (Parkhurst and Appelo, 2013).

595 The water composition in equilibrium with the identified set of minerals was
596 reconstructed to represent the water in the reservoir before halite dissolution starts. To
597 do that, equimolar amounts of chloride and sodium were subtracted from the solution,
598 down to Cl^- = 0 mol/L, while maintaining the other mineral equilibria (albite, K-
599 feldspar, quartz, anhydrite, calcite and dolomite) at the reservoir temperature (82 ºC in
600 the case of the high-sulphate group and 95 ºC in the case of the low-sulphate group).
601 From this theoretical solution, the effects of increasing the concentrations of chloride
602 (and Na, through halite dissolution) on the rest of the chemical components controlled
603 by the imposed mineral equilibria, can be discussed. The results obtained for all the
604 samples are similar and therefore, only those from T3 are shown in Figure 7.

605 The theoretical evolution of the concentration of the major elements in sample T3 is
606 plotted in Figures 7a to 7d against chloride under the situation of equilibrium with the
607 rest of the mineral set. The concentration of all these major elements (Na, K, Ca, Mg
608 and sulphate), although controlled by that equilibrium situation at a constant
609 temperature, increases with sodium and chloride (except for silica whose concentrations
610 is almost constant, Figure 7b).

611 Dissolved sulphate increases with chloride contents (Figure 7d) as anhydrite solubility
612 is enhanced by the increase of salinity and, therefore, by halite dissolution:

613 $$NaCl_{(hal)} + CaSO_{4(anh)} \rightarrow Na^+ + Cl^- + Ca^{2+}\, SO_4^{2-} \quad (1)$$

614 The increase in dissolved sodium promotes, in turn, the displacement of the albite-K-
615 feldspar equilibrium reaction towards the left, increasing the amount of dissolved
616 potassium (Figure 7c):

617 $$NaAlSi_3O_{8(alb)} + K^+ \leftrightarrow KAlSi_3O_{8(K-feld)} + Na^+ \quad (2)$$

And the increase of dissolved calcium promotes the displacement of the calcite-dolomite equilibrium reaction towards the left, increasing the concentrations of dissolved magnesium (Figure 7b):

$$2CaCO_{3(calc)} + Mg^{2+} \leftrightarrow CaMg(CO_3)_{2(dol)} + Ca^{2+} \quad (3)$$

The two last panels in Figure 7 (e and f) show the evolution of the elemental ratios Ca/Mg and Na/K. The corresponding activity ratios stay constant under the specific temperature in the calculations as they are controlled by the calcite-dolomite and albite-K-feldspar equilibria, respectively (reactions 2 and 3); however, the elemental ratios show a different behaviour. The Na/K elemental ratio is also constant and near the corresponding activity ratio (aNa^+/aK^+ = 185) because these elements are almost unaffected by complexing and the free ion activity coefficients mutually cancel out (Chiodini et al., 1991). The Ca/Mg elemental ratio, however, is different from the activity ratio (aCa^{2+}/aMg^{2+} = 1.59) and slightly increases with Cl^- concentrations (Figure 7e; note the vertical scale) as these elements are more and differentially affected by the effect of complexation and activity coefficient calculations, which cause a deviation between the total contents and the activities (Chiodini *et al.*, 1991).

These results indicate that although the chemistry of the waters is mainly controlled by mineral equilibria at a given temperature, the concentration of mobile elements are, therefore, an important variable in the control of the water composition. In the case studied here, the mobile element participating in the control of the system is chloride. Nonetheless, in other systems in which sulphate is not controlled by equilibrium with anhydrite or gypsum, the concentration of this component may have an influence in the controlled elements of the waters.

5.2. *Effects of the chemical characteristics of the water in a future CO_2 storage*

During the ALGECO2 project (IGME, 2010), a favourable tectonic and sedimentary structure for CO_2 storage was identified in the studied area (the Leyre-Berdún structure; Suárez *et al.*, 2014) in the Paleocene-Eocene carbonate rocks, which probably is the aquifer of the Tiermas thermal waters. If the features of the waters in that structure are similar to those deduced in the thermal waters, then some important conclusions about some plausible processes effective during the CO_2 injection could be drawn. For example, in the vicinity of the injection well, the desiccation of the saline waters in contact with dry CO_2 could easily induce the precipitation of carbonates and sulphates (Gaus, 2010; Gimeno et al., 2011; Gutierrez et al., 2011) as the waters at depth are in equilibrium with calcite, dolomite and anhydrite. In the long term, injection of CO_2 will promote the acidification of the saline groundwaters, which will lead to the dissolution of carbonate minerals (calcite and dolomite). In this context, precipitation of sulphates (gypsum or anhydrite) may be triggered as the waters are in equilibrium with anhydrite (e.g. with high concentrations of dissolved sulphate). A similar situation has been found in the Spanish test site for CO_2 geological storage, located at Hontomin (Burgos), in a limestone reservoir, also with sulphate-rich saline groundwaters in equilibrium with gypsum/anhydrite (García-Ríos et al., 2014).

These processes involving carbonate and sulphate minerals are kinetically fast and their effects on the porosity and permeability of the reservoir rocks or in the well environment should be evaluated in future and more detailed site selection studies.

6. Conclusions

Two hydrogeochemical groups of waters have been identified in Tiermas springs: a group with TDS about 7,500 ppm and low sulphate contents (low-sulphate group) and other with TDS close to 11,000 ppm and higher sulphate contents (high-sulphate group).

The temperature of the waters in the reservoir has been determined by combining various chemical and isotopic geothermometers with geothermometrical modelling, and a reliable range of temperatures has been established. The temperatures predicted for the waters are also slightly different for each group; being 90 ± 20 ºC for the low-sulphate group and slightly lower 82 ± 15 ºC for the high-sulphate one.

It is remarkable the good results obtained with some cationic geothermometers, such as the Na/K geothermometer, in a geothermal system of low temperature and hosted in carbonate-evaporitic rocks like the studied here. This unusual situation may be attributed to the presence of detrital rocks (silicate minerals) in the carbonate-evaporitic aquifer, which provides for equilibrium between albite and K-feldspar as found in the geothermometrical modelling.

The two water groups are in equilibrium with the same mineral assemblage in the reservoir (calcite, dolomite, quartz, anhydrite, albite, K-feldspar and other aluminosilicate phases). However they show slight differences in the temperature at depth and in the concentration of some chemical elements, which suggests that each group of waters could represent a different flow path with different types and/or intensities of water-rock interaction processes.

The influence of halite dissolution has also been evaluated and the results indicate that apart from temperature, chloride contents of the thermal waters have a significant influence on the concentrations of SO_4, Na, K, Ca and Mg measured in these waters. As

688 demonstrated in the simulations presented here, if halite dissolution had occurred during
689 the ascent of the thermal waters (without the influence of the mineral equilibria at
690 depth) their chemical characteristics would be different. These results, along with the
691 fact that anhydrite is included in the mineral assemblage in equilibrium in the reservoir,
692 indicate that the waters should be in contact with an evaporitic facies in the reservoir
693 and not during their ascent to surface.

694 Finally, as a favourable structure for CO_2 storage has recently been identified in the
695 Paleocene-Eocene carbonates, the probable aquifer of the Tiermas geothermal system,
696 the groundwaters studied here could be used as analogues to the waters in that site.
697 Therefore, the results of this study are useful for understanding the main processes
698 related to the CO_2 injection and mixing with this type of water. Near the injection wells,
699 the waters will desiccate causing the precipitation of calcite, dolomite and anhydrite,
700 since the waters are in equilibrium with respect to these phases in the reservoir,
701 affecting the porosity and permeability of the rocks. And in the long term, the water will
702 acidify leading to the carbonate dissolution and sulphate precipitation.

703 ## 7. Acknowledgements

704 M. Blasco is working in this study thanks to a scholarship from the Ministry of
705 Education, Culture and Sports of Spain, for the Training of University Teachers (ref.
706 FPU14/01523). This study forms part of the activities of the Geochemical Modelling
707 Group (University of Zaragoza; Aragón Government). The comments of Dr. M.H. Reed
708 and of an anonymous reviewer have contributed to improve the work and are gratefully
709 appreciated.

710 ## 8. References

711 Appelo, C.A.J. and Postma, D. (2005). *Geochemistry, Groundwater and Pollution*. 2nd
712 Edition. Rotterdam: A.A. Balkema.

713 Arnorsson, S., Gunnlaugsson, E. and Svavarsson, H. (1983). The chemistry of
714 geothermal waters in Iceland. III. Chemical geothermometry in geothermal
715 investigations. *Geochimica et Cosmochimica Acta*, **47**, 567-577.

716 Asta, M.P, Gimeno, M.J., Auqué, L.F., Gómez, J., Acero, P. and Lapuente, P. (2010).
717 Secondary processes determining the pH of alkaline waters in crystalline rock
718 systems.*Chemical Geology*, **276**, 41-52.

719 Auqué, L.F. (1993). Estudio de sistemas geotermales en Aragón. Pautas de especiación
720 y reacción aplicadas a la modelización de sistemas de baja - media entalpía.
721 Doctoral Thesis. Zaragoza, Spain: University of Zaragoza.

722 Ayora, C., Garcia-Veigas, J. and Puevo, J. (1994). The chemical and hydrological
723 evolution of an ancient potash-forming evaporite basin as constrained by mineral
724 sequence, fluid inclusion compostion and numerical simulation. *Geochimica et*
725 *Cosmochimica Acta*, **58**, 3779-3794.

726 Ayora, C., Taberner, C., Pierre, C. and Pueyo J.J. (1995). Modeling the sulfur and
727 oxygen isotopic composition of sulfates through a halite-potash sequence:
728 Implications for the hydrological evolution of the Upper Eocene South Pyrenean
729 Basin. *Geochimica et Cosmochimica Acta*, **59**, 1799 - 1808.

730 Awaleh, M.O., Hoch, F.B., Boschetti, T., Soubaneh, Y.D., Egueh, N.M, Elmi, S.K.,
731 Mohamed, J. and Khaireh, M.A. (2015). The geotermal resources of the
732 Republic of Djibouti - II: Geochemical study of the Lake Abhe geothermal field.
733 *Journal of Geochemical Exploration*, **159**, 129-147.

734 Baeza, J., Torreano, R. and Cerezuela, M.A. (2000). Estudio para caracterizar, evaluar y
735 proteger las aguas minerales y termales de una comunidad: Aragón. In: J.A.
736 López Geta and J.L. Pinuaga (Eds.), *Panorama actual de las aguas minerales y*
737 *minero-medicinales en España.* Madrid: Instituto Geológico y Minero de España
738 (IGME). pp. 283-303.

739 Bauluz, B., González, J.M., Yuste, A. and Mayayo, M.J. (2008). Evolución Diagenética
740 de las Turbiditas del Grupo Hecho (Eoceno) en la Cuenca de Jaca (España).
741 *Revista de la sociedad española de mineralogía (Macla)*, **9**, 47-48.

742 Boschetti, T. (2013). Oxygen isotope equilibrium in sulfate-water systems: A revisión
743 of geothermometric applications in low-enthalpy systems. *Journal of*
744 *Geochemical Exploration*, **124**, 92-100.

745 Boschetti, T., Giampiero, V., Toscani, L., Barbieri, M. and Mucchino, C. (2005). The
746 Bagni di Lucca termal waters (Tuscany, Italy): an example of Ca-SO_4 waters
747 with high Na/Cl and low Ca/SO_4 ratios. *Journal of Hydrology*, **307**, 270-293.

748 Boschetti, T., Cortecci, G., Toscani, L. and Iacumin, P. (2011). Sulfur and oxygen
749 isotope compositions of Upper Triassic sulfates from northern Apennines (Italy):
750 paleogeographic and hydrogeochemical implications. *Geologica Acta*, **9** (2),
751 129-147.

752 Brenninkmeijer, C.A.M., Kraft, P. and Mook, W.G. (1983). Oxygen isotope
753 fractionation between CO_2 and H_2O. *Isotope Geoscience*, **1**, 181-190.

754 Chiba, H., Kusakabe, M., Hirano, S.I, Matsuo, S. and Somiya, A. (1981). Oxygen
755 isotope fractionation factors between anhydrite and water from 100 to 550°C.
756 *Earth and Planetary Science Letters*, **53**, 55-62.

Chiodini, G., Cioni, R., Guidi, M. and Marini, L. (1991). Chemical geothermometry and geobarometry in hydrothermal aqueous solutions: A theoretical investigation based on a mineral-solution equilibrium model. *Geochimica et Coscmochimica Acta*, **55**, 2709-2727.

Chiodini, G., Frondini, F. and Marini, L. (1995). Theoretical geothermometers and pCO_2 indicators for aqueous solutions coming from hydrothermal systems of medium-low temperature hosted in carbonate-evaporite rocks. Application to the thermal springs of the Etruscan Swell. Italy. *Applied Geochem*istry, **10**, 337-346.

Clark, I. and Fritz, P. (1997). *Environmental Isotopes in Hydrogeology*. Boca -Raton (Florida): CRC Press/Lewis Publishers.

Consulnima S.L. (2011). *Informe piezómetro de Romanzado: 090.031.001*. Inspección y vigilancia de las obras de Construcción de sondeos para la Adecuación de las Redes de Piezometría y Calidad de las Aguas Subterráneas. Cuenca del Ebro. Zaragoza: Confederación Hidrográfica del Ebro.

Craig, H. (1961). Isotopic variations in meteoric waters. *Science,* **133**, 1702-1703.

D´Amore, F., Fancelli, R. and Caboi, R. (1987). Observations of the application of chemical geothermometers to some hydrothermal systems in Sardinia. *Geothermics*, **16**, 271-282.

D'Amore F. and Arnórsson S. (2000). Geothermometry. In: Arnórsson S., (Ed.), *Isotopic and chemical techniques in geothermal exploration, development and use* (pp. 152-199). Vienna: International Atomic Agency.

778 Deines, P., Languir, D. and Harmon, R.S. (1974). Stable carbon isotope ratios and the
779 existence of a gas phase in the evolution of carbonate ground water. *Geochimica*
780 *et Cosmochimica Acta*, **38**, 1147-1168.

781 Díaz-Teijeiro, M. F., Rodríguez-Arévalo, J. and Castaño, S (2009). La Red Española de
782 Vigilancia de Isótopos en la Precipitación (REVIP): distribución isotópica
783 espacial y aportación al conocimiento del ciclo hidrológico. *Ingeniería Civil*,
784 **155**, 87-97.

785 Faci, E. (Dir.) (1997). *Cartografía Geológica de Navarra. E, 1:25000. Hoja 175-I:*
786 *Tiermas.* Navarra: Gobierno de Navarra. Departamento de Obras Públicas,
787 Transportes y Comunicaciones.

788 Fernández, J., Auqué, L.F. Sánchez Cela, V.S. and Guaras, B. (1988). Las aguas
789 termales de Fitero (Navarra) y Arnedillo (Rioja). Análisis comparativo de la
790 aplicación de técnicas geotermométricas químicas a aguas relacionadas con
791 reservorios carbonatado-evaporíticos. *Estudios geológicos*, **44**, 453-469.

792 Fournier, R.O. (1977). Chemical geothermometers and mixing models for geothermal
793 systems. *Geothermics*, **5**, 41-50.

794 Fournier, R.O. (1979). A revised equation for the Na-K geothermometer. *Geothermal*
795 *Resources Council Transactions*, **3**, 221-224.

796 Fournier, R.O. (1982). Water geothermometers applied to geothermal energy. In: (F.
797 D'Amore, Co-ordinator) *Applications of Geochemistry in Geothermal reservoir*
798 *Development*. UNITAR/UNDO centre on Small Energy Resources: Rome. pp.
799 37-69.

Fournier, R.O. and Truesdell, A.H. (1973). An empirical Na-K-Ca geothermometer for natural waters. *Geochimica et Cosmochimica Acta*, **37**, 1255-1275.

Fournier, R.O. and Potter, R.W. (1982). An equation correlating the solubility of quartz in water from 25 to 900°C at pressures up to 10000 bars. *Geochimica et Cosmochimica Acta*, **46**, 1975-1978.

Friedman, I. and O'Neil, J.R. (1977). Compilation of stable isotope fractionation factors of geochemical interest. In: M. Fleischer (Ed.), *Data on Geochemistry* (6^{th} ed.). Chapter KK. USGS Professional Paper 440-KK. Washington: United States Government Printing Office.

Garcia-Rios, M., Cama, J., Luquot, L. and Soler, J.M. (2014). Interaction between CO_2-rich sulfate solutions and carbonate reservoir rocks from atmospheric to supercritical CO_2 conditions: Experiments and modeling. *Chemical Geology*, **383**, 107-122.

Gaus, I. (2010). Role and impact of CO_2-rock interactions during CO_2 storage in sedimentary rocks. *International Journal of Greenhouse Gas Control*, **4**, 73-89.

Giggenbach, W., Gonfiantini, R., Jangi, B.L. and Truesdell, A.H. (1983). Isotopic and chemical composition of Parbati valley geothermal discharges, N.W. Himalaya. India. *Geothermics*, **12**, 199‑222.

Giggenbach, W.F. (1988). Geothermal solute equilibria. Derivation of Na-K-Mg-Ca geoindicators. *Geochimica et Cosmochimica Acta*, **52**, 2749-2765.

Gimeno, M.J., Acero, P., Gutiérrez, V, Auqué, L.F., Asta, M.P. & Gómez, J.B. (2011). Evaluation of thermodynamic data and activity coefficient models for the

822 geochemical modeling of CO_2 storage systems. *Mineralogical Magazine*, 75(3):
823 918.

824 Grimaud, D,, Beaucaire, C. and Michard, G. (1990). Modelling of the evolution of
825 ground waters in a granite system at low temperature: the Stripa ground waters,
826 Sweden. *Applied Geochemistry*, **5**, 515-525.

827 Gupta, K.D. and Pickering, K. T. (2008). Petrography and temporal changes in
828 petrofacies of deep-marine Aínsa-Jaca basin sandstone systems, Early and
829 Middle Eocene, Spanish Pyrenees. *Sedimentology*, **55**, 1083-1114.

830 Gutiérrez, V., Acero, P., Auqué, L.F., Gimeno, M.J. (2011). Modelización geoquímica
831 de la evolución del entorno de un pozo de inyección de CO_2 y evaluación de
832 condicionantes termodinámicos. *Macla*, 15.

833 Halas, S. and Pluta, I. (2000). Empirical calibration of isotope thermometer $\delta^{18}O$
834 (SO_4^{2-})-$\delta^{18}O$ (H_2O) for low temperature brines, In: *V Isotope Workshop*.
835 Kraków, Poland. pp. 68-71.

836 Hanor, J.S. (1994). Physical and chemical controls on the composition of waters in
837 sedimentary basins. *Marine and Petroleum Geology*, **11**, 31-45.

838 Hanor, J.S. (1996). Variations of chloride as a driving force in siliciclastic diagenesis.
839 *Siliciclastic Diagenesis and Fluid Flow: Concepts and applications, SEPM*
840 *Special Publication*, **55**, 3-12.

841 Hanor, J.S. (2001). Reactive transport involving rock-buffered fluids of varying
842 salinity. *Geochmica et Cosmochimica Acta*, **65**, 3721-3732.

Helgeson, H.C. (1970). Description and interpretation of phase relations in geochemical processes involving aqueous solutions. *American Journal of Science*, **268**, 415-438.

Helgeson, H.C., Delany, J.M., Nesbitt, H.W. and Bird, D.K. (1978). Summary and critique of the thermodynamic properties of rock-forming minerals. *American Journal of Science*, **278ª**.

IGME (1973). *Mapa Geológico de España. E. 1:50000. Hoja 175: Sigües.* Madrid: Instituto Geológico y Minero de España (IGME).

IGME (2010). Selección y caracterización de áreas y estructuras geológicas favorables para el almacenamiento geológico de CO_2 en España. http://info.igme.es/algeco2/ (accessed 21-03-2016).

ITGE-DGA (1994). Estudio de las aguas minero-medicinales, minero-industriales, termales y de bebida envasada en la Comunidad Autónoma de Aragón. Madrid: Instituto Geológico y Minero de España (IGME).

Jiménez, M. (1838). *Tratado de materia farmacéutica* (2ª ed.). Madrid: Imprenta de la Viuda de Sanchiz e hijos.

Kharaka, Y.K. and Mariner, R.H. (1989). *Chemical geothermometers from water-mineral equilibria*. In: Abstracts of the 28th International Geological Congress (vol. 2), Washington D.C. pp. 184-185.

Larrasoaña, J.C., Pueyo, E.I., del Valle, J., Millán, H., Pocoví, A. and Dinarés, J. (1996). Datos magnetotectónicos del Eoceno de la Cuenca de Jaca - Pamplona: resultados iniciales. *Geogaceta,* **30**, 1058-1061.

865 Lloyd, R.M. (1968). Oxygen isotope behaviour in the sulfate-water system. *Journal of*
866 *Geophysical Research*, **73**, 6099-6110.

867 López-Chicano, M., Cerón, J.C., Vallejos, A. and Pulido-Bosch, A. (2001).
868 Geochemistry of thermal springs, Alhama de Granada (southern Spain). *Applied*
869 *Geochemistry*, **16**, 1153-1163.

870 Marini, L. (2004). *Geochemical techniques for the exploration and exploitation of*
871 *geothermal energy*. Genova: Laboratorio di Geochimica, Università degli Studi
872 di Genova.

873 Marini, L. Chidioni, G. and Cioni, R. (1986). New geothermometers for carbonate-
874 evaporite geothermal reservoirs. *Geothermics*, **15**, 77-86.

875 Marini, L., Bonaria, V., Guidi, M., Hunziker, J.C., Ottonello, G., and Vetuschi
876 Zuccolini, M. (2000). Fluid geochemistry of the Acqui Terme-Visone
877 geothermal area (Piemonte, Italy). *Applied Geochemistry*, **15**, 917-935.

878 Merino, E. and Ramson, B. (1982). Free energies of formation of illite solid solutions
879 and their compositional dependence. *Clays and Clay Minerals*, **30**, 29-39.

880 Mey, P.H.W., Nagtegaal, P.J.C., Roberti, K.J. and Hartevelt, J.J.A. (1968).
881 Lithostratigraphic subdivision of post-hercynian deposits in the south-central
882 Pyrenees, Spain. *Leidse Geologische Mededelingen*, **41**, 221-228.

883 Michard, G. (1979). Géothermomètres chimiques. B.R.G.M. (2nd Ser.), section III, **2**,
884 183-189.

885 Michard, G. (1987). Controls of the chemical composition of geothermal waters. In:
886 H.C. Helgeson (ed.), *Chemical Transport in Metasomatic Processes* (pp. 323-
887 353). Dordrecht (Netherlands): D. Reidel Publishing Company.

888 Michard, G. and Fouillac, C. (1980). Contrôle de la composition chimique des eaux
889 thermals sulfurées sodiques du Sud de la France. In: Tardy, Y. (Ed.),
890 *Geochimique des interactions entre les eaux, les minéraux et les roches*.
891 Elements: Tarbes, pp. 147-166.

892 Michard, G. and Roekens, E. (1983). Modeling of the chemical composition of alkaline
893 hot waters. *Geothermics*, **12**, 161-169.

894 Michard, G., Sanjuan, B., Criaud, A., Fouillac, C., Pentcheva, E.N., Petrov, P.S. and
895 Alexieva, R. (1986). Equilibra and geothermometry in hot waters from granites
896 of SW Bulgaria. *Geochemical Journal*, **20**, 159-171.

897 Michard, G. and Bastide, J.P. (1988). Etude Geochimique de la nappe du Dogger du
898 Bassin Parisien. *Journal of Volcanology and Geothermal Research*, **35**, 151-163.

899 Michard, G., Pearson, F.J.Jr. and Gautschi, A. (1996). Chemical evolution of waters
900 during long term interaction with granitic rocks in northern Switzerland. *Applied*
901 *Geochemistry*, **11**, 757-774.

902 Mizutani, Y. and Rafter, T.A. (1969). Oxygen isotopic composition of sulphates. 3.
903 Oxygen isotopic fractionation in the bisulfate ion-water system. *New Zeland*
904 *Journal of Science*, **12**, 54-59.

905 Mook, W.G., Bommerson, J.C. and Staverman, W.H. (1974). Carbon isotope
906 fractionation between dissolved bicarbonate and gaseous carbon dioxide. *Earth*
907 *and Planetary Science Letters*, **22**, 169-176.

908 Nordstrom, D.K., Ball, J.W., Donahoe, R.J. and Whittemore, D. (1989). Groundwater
909 chemistry and water-rock interactions at Stripa. *Geochimica et Cosmochimica*
910 *Acta*, **53**, 1727-1740.

911 Nordstrom, D. K., Plummer, L. N., Langmuir, L., Busenberg, E., May, H. M., Jones, B.
912 F. and Parkhurst, D. L. (1990). Revised chemical equilibrium data for major
913 water-mineral reactions and their limitation. In: Melchior, D.C. and Basset, R.L.
914 (Eds.), *Chemical Modeling of Aqueous Systems II*. Symposium Series 416.
915 Washington DC: American Chemical Society. pp. 398-413.

916 Oliva, B., Millán, H., Pocoví, A. and Casas A.M. (1996). Estructura de la Cuenca de
917 Jaca en el sector occidental de las Sierras Exteriores Aragonesas. *Geogaceta,* **20**,
918 800-802.

919 Olivia-Urcia, B., Casas, A.M., Pueyo, E.L. and Pocoví-Juan, A. (2012). Structural and
920 paleomagnetic evidence for non-rotanional kinematics of the South Pyrenean
921 Frontal Thrust at the western termination of the External Sierras (southwestern
922 central Pyrenees). *Geologica Acta*, **10**, 125-144.

923 O'Neil, J.R. and Adami, L. H. (1969). The oxygen isotope partition function ratio of
924 water and the structure of liquid water. *Journal of Physical Chemistry*, **73** (5),
925 1553-1558.

926 Palandri, J.L. and Reed M.H. (2001). Reconstruction of in situ composition of
927 sedimentary formation waters. *Geochimica et Cosmochimica Acta*, **65**, 1741-
928 1767.

929 Pang, Z. and Reed, M.H. (1998). Theoretical chemical thermometry on geothermal
930 waters: Problems and methods. *Geochimica et Cosmochimica Acta*, **62**, 1083-
931 1091.

932 Parkhurst, D.L. and Appelo, C.A.J. (2013). Description of Input and Examples for
933 PHREEQC Version 3. A Computer Program for Speciation, Batch-Reaction,
934 One-Dimensional Transport, and Inverse Geochemical Calculations. In: U.S.

935 Geological Survey (Ed.). *Techniques and Methods, book 6, chap. A43*, Denver,
936 Colorado: U.S.G.S., available only at http://pubs.usgs.gov/tm/06/a43.

937 Pastorelli, S., Marini, L. and Hunziker, J.C. (1999). Water chemistry and isotope
938 composition of the Acquarossa thermal system, Ticino, Switzerland.
939 *Geothermics*, **28**, 75-93.

940 Payros, A., Orue-Etxebarria, X., Bacera, J.I. and Pujalte, V. (1994). Las
941 "megaturbiditas" y otros depósitos de resedimentación carbonatada a gran escala
942 del Eoceno surpirenaico: nuevos datos del área Urrobi-Ultzama (Navarra).
943 *Geogaceta*, **16**, 94-97.

944 Peiffer, L., Wanner, C., Spycher, N., Sonnenthal, E.L., Kennedy, B.M., Iovenitti, J.
945 (2014). Optimized multicomponent vs. classical geothermometry: Insights from
946 modeling studies at the Dixie Valley geothermal area. *Geothermics*, **51**, 154-
947 169.

948 Pueyo, E.L., Calvin, P., Casas, A.M., Olivia-Ucria, B., Klimowitz, J., Garcia-Lobón,
949 J.L., Rubio, F.M., Ibarra, P.I., Martínez-Duran, P., Rey-Moral, M.C., Pérez, I.
950 and Martín, J. M. (2012). A research plan for a large potential CO_2 reservoir in
951 the Southern Pyrenees. *Geotemas*, **13**, 1970-1973.

952 Puigdefàbregas, C. (1975). La sedimentación molásica en la cuenca de Jaca. *Pirineos*,
953 **104**.

954 Reed, M. and Spycher, N. (1984). Calculation of pH and mineral equilibria in
955 hydrothermal waters with application to geothermometry and studies of boiling
956 and dilution. *Geochimica et Cosmochimica Acta*, **48**, 1479-1492.

957 Sáenz, C. (1999). *Patrimonio geológico del Camino de Santiago.* Madrid: Instituto
958 Tecnológico GeoMinero de España.

959 Sánchez Guzmán, J. and García de la Noceda, C. (2005). *Geothermal Energy*
960 *Development in Spain - Country Update Report*. In: Proceedings World
961 Geothermal Congress 2005. Antalya, Turkey. pp. 1-10

962 Sánchez, J.A. (2000). *Las aguas termales en Aragón: Estudio hidrogeotérmico.*
963 Zaragoza: Consejo de Protección de la Naturaleza de Aragón.

964 Sánchez, J.A., Coloma, P., Pérez-García, A. and De Leiva, A. (2000). Evaluación del
965 flujo geotérmico en manantiales de Aragón. *Geogaceta*, **27**, 155-158.

966 Sánchez, J.A., Colom, P. and Pérez-García, A. (2004). Evaluation of geothermal flow at
967 the springs in Aragón (Spain), and its relation to geologic structure.
968 *Hydrogeology Journal*, **12**, 601-609.

969 Saura, E. and Teixell, A. (2006). Inversion of small basins: effects on structural
970 variations at the leading edge of the Axial Zone antiformal stack (Southern
971 Pyrenees, Spain). *Journal of Structural Geology*, 28, 1909-1920.

972 Seal, R.R.I., Alpers, C.N. and Rye, R.O. (2000). Stable isotope systematics of sulfate
973 minerals. In: C.N. Alpers, J.L. Jambor, and D.K Nordstrom, D.K. (Eds.), *Sulfate*
974 *Minerals — Crystallography: Geochemistry and Environmental Significance*
975 (pp. 541-602). Chantilly (Virginia): Mineral Society of America.

976 Spycher, N., Peiffer, L., Sonnenthal, E.L., Saldi, G., Reed, M.H.; Kennedy, B.M.
977 (2014). Integrated multicomponent solute geothermometry. *Geothermics*, **51**,
978 113-123.

979 Suárez, I., Arenillas, A., Medaito, J.F., García, J., Molinero, R. and Catalina, R. (2014).
980 *Atlas de estructuras del subsuelo susceptibles de almacenamiento geológico de*
981 *CO_2 en España.* Madrid: Instituto Geológico y Minero de España (IGME).
982 Instituto para la Reestructuración de la Minería del carbón y desarrollo
983 Alternativo de las Comarcas Mineras.

984 Tole, M.P., Armannsson, H., Pang, Z. and Arnorsson, S. (1993). Fluid/mineral
985 equilibrium calculations for geothermal fluids and chemical geothermometry.
986 *Geothermics*, **22**, 17-37.

987 Trotignon L., Beaucaire, C., Louvat, D. and Aranyossy, J.F. (1999). Equilibrium
988 geochemical modelling of Äspö groundwaters: a sensitivity study of
989 thermodynamic equilibrium constants. *Applied Geochemistry*, **14**, 907-916.

990 Truesdell, A.H. (1974) Oxygen isotope activities and concentrations in aqueous salt
991 solutions at elevated temperatures: Consequences for isotope geochemistry.
992 *Earth Planet Science Letters*, **23**, 387-396.

993 Truesdell, A.H. (1976). *Geochemical Techniques in Exploration*. Summary of Section
994 III. In: Proceedings of the Second United Nations Symposium on the
995 Development and Use of Geothermal Resources. San Francisco, California. pp.
996 iii-xxix

997 Utrilla, R., Pierre, C., Ortí, F., Rosell, L., Inglés, M. and Pueyo, J.J. (1987). *Estudio*
998 *isotópico de los sulfatos en formaciones evaporíticas mesozoicas y terciarias*
999 *continentales*. In: II Congreso de Geoquímica de España. Soria. pp. 91-94.

1000 Wang, J., Jin, M., Jia, B. and Kang, F. (2015). Hydrochemical characteristics and
1001 geothermometry applications of thermal groundwater in northern Jinan,
1002 Shandong, China. *Geothermics*, **57**, 185-195.

Zeebe, R.E. (2010). A new value for the stable oxygen isotope fractionation between dissolved sulfate ion and water. *Geochimica et Cosmochimica Acta*, **74**, 818-828.

Zheng, Y.F. (1999). Oxygen isotope fractionation in carbonate and sulfate minerals. *Geochemical Journal*, **33**, 109-126.

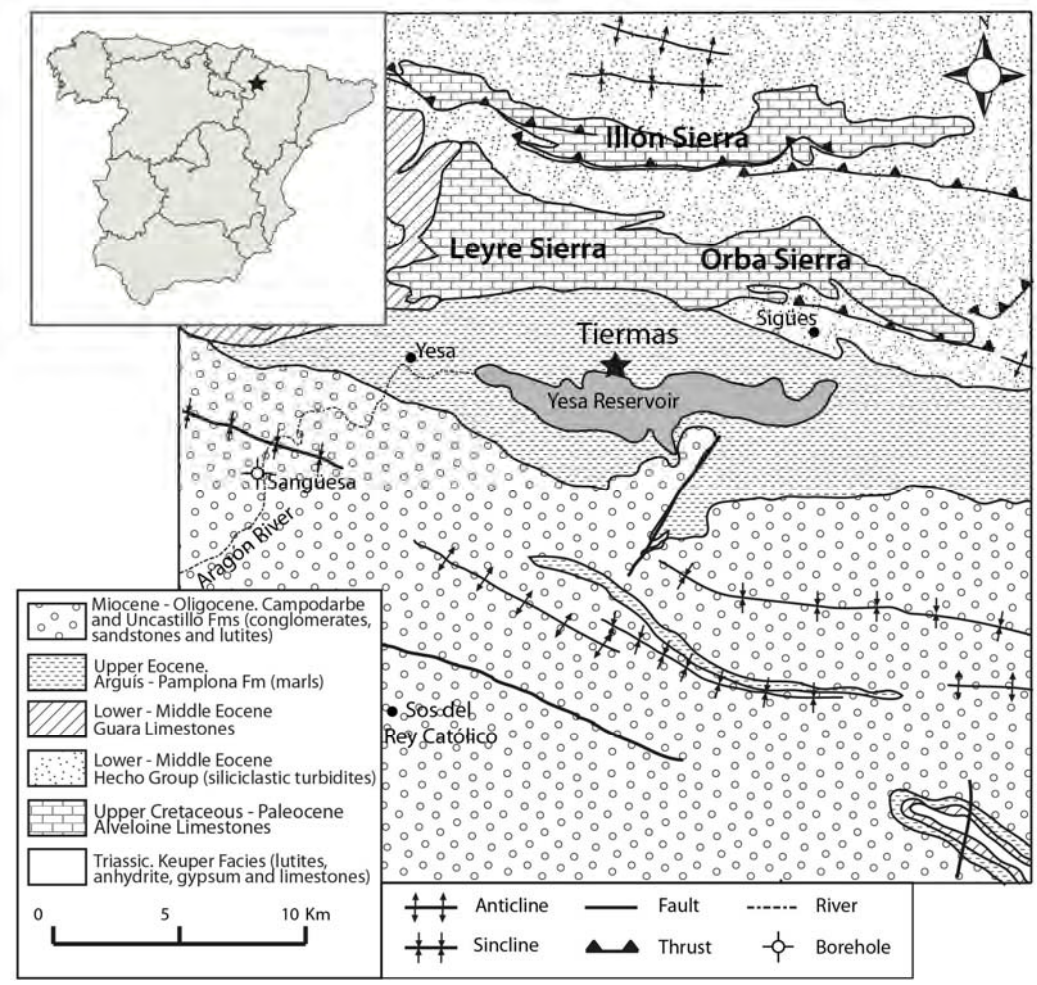

1023

1024 Figure 1

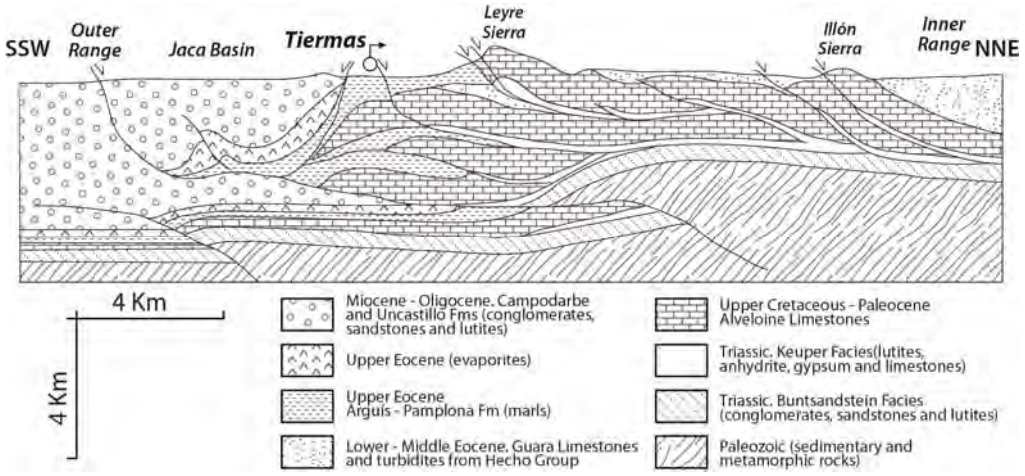

1025

1026 Figure 2

1027

1028

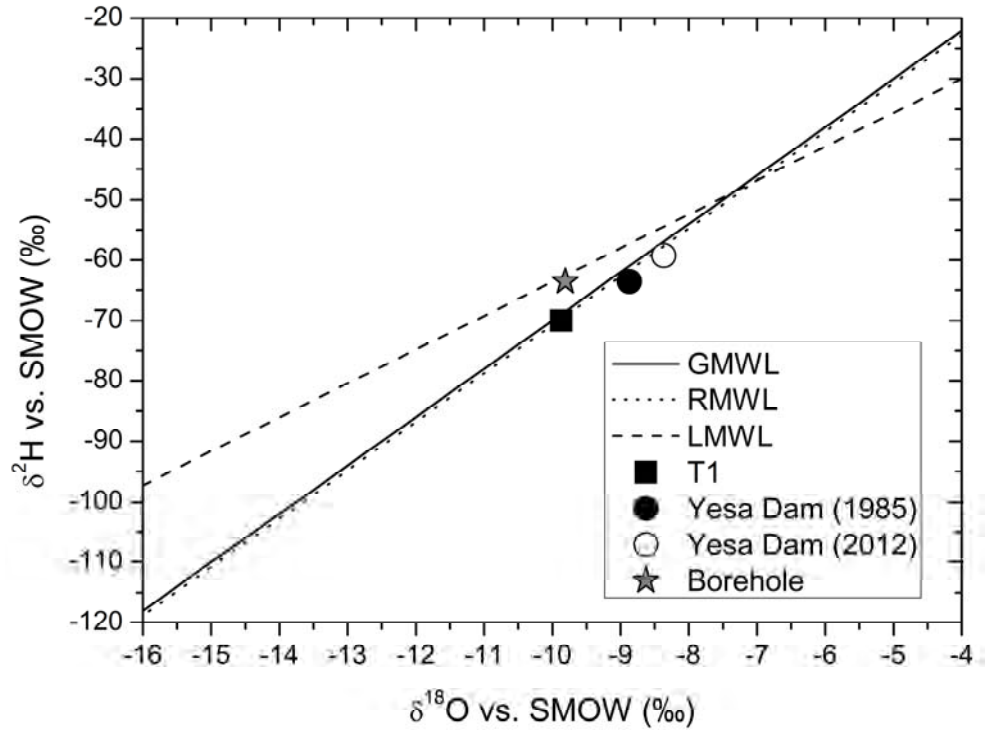

1029

1030 Figure 3

1031

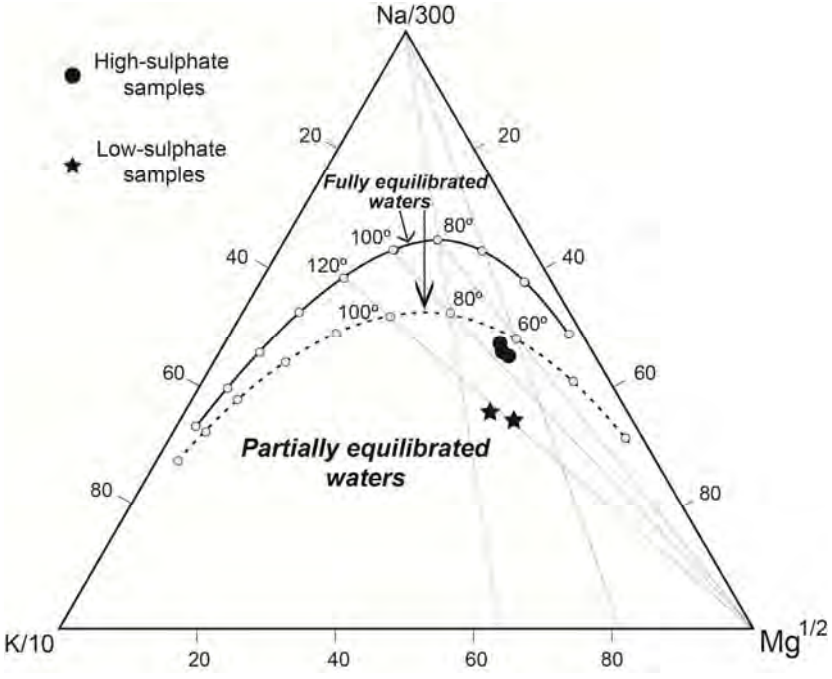

1032

1033 Figure 4

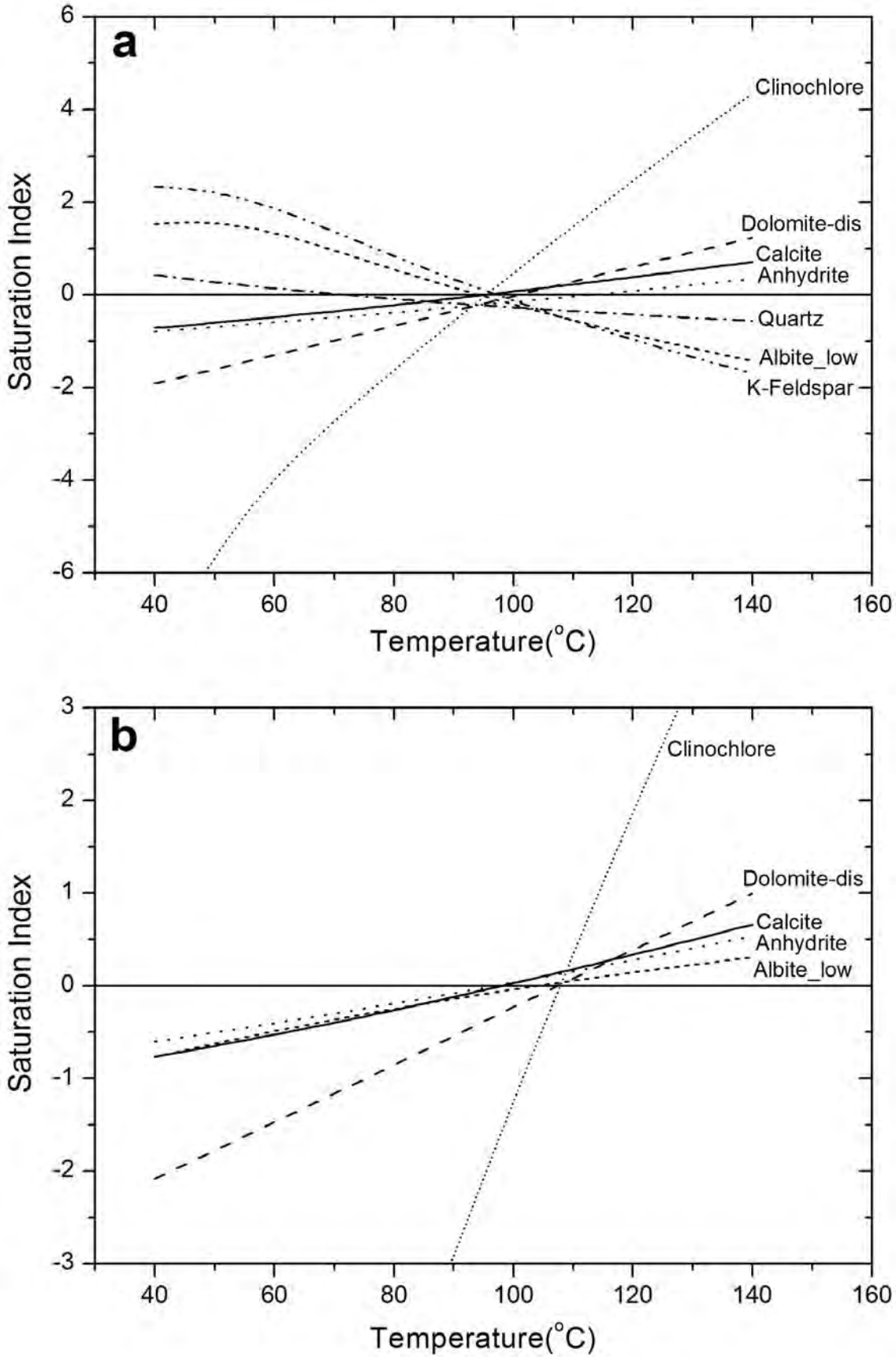

1034

1035 Figure 5

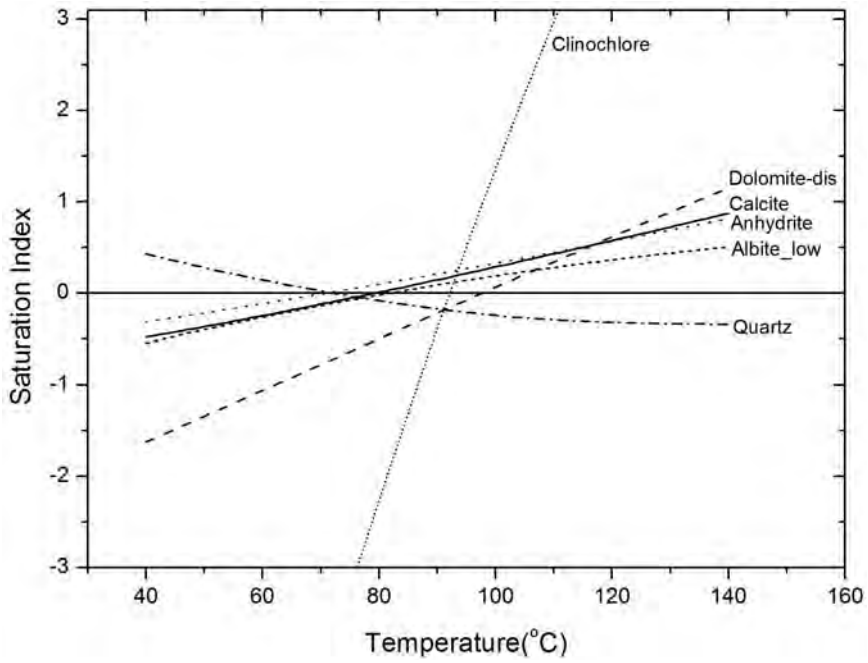
Clinochlore
Dolomite-dis
Calcite
Anhydrite
Albite_low
Quartz
Saturation Index
Temperature(°C)
3
2
1
0
-1
-2
-3
40
60
80
100
120
140
160

Figure 6

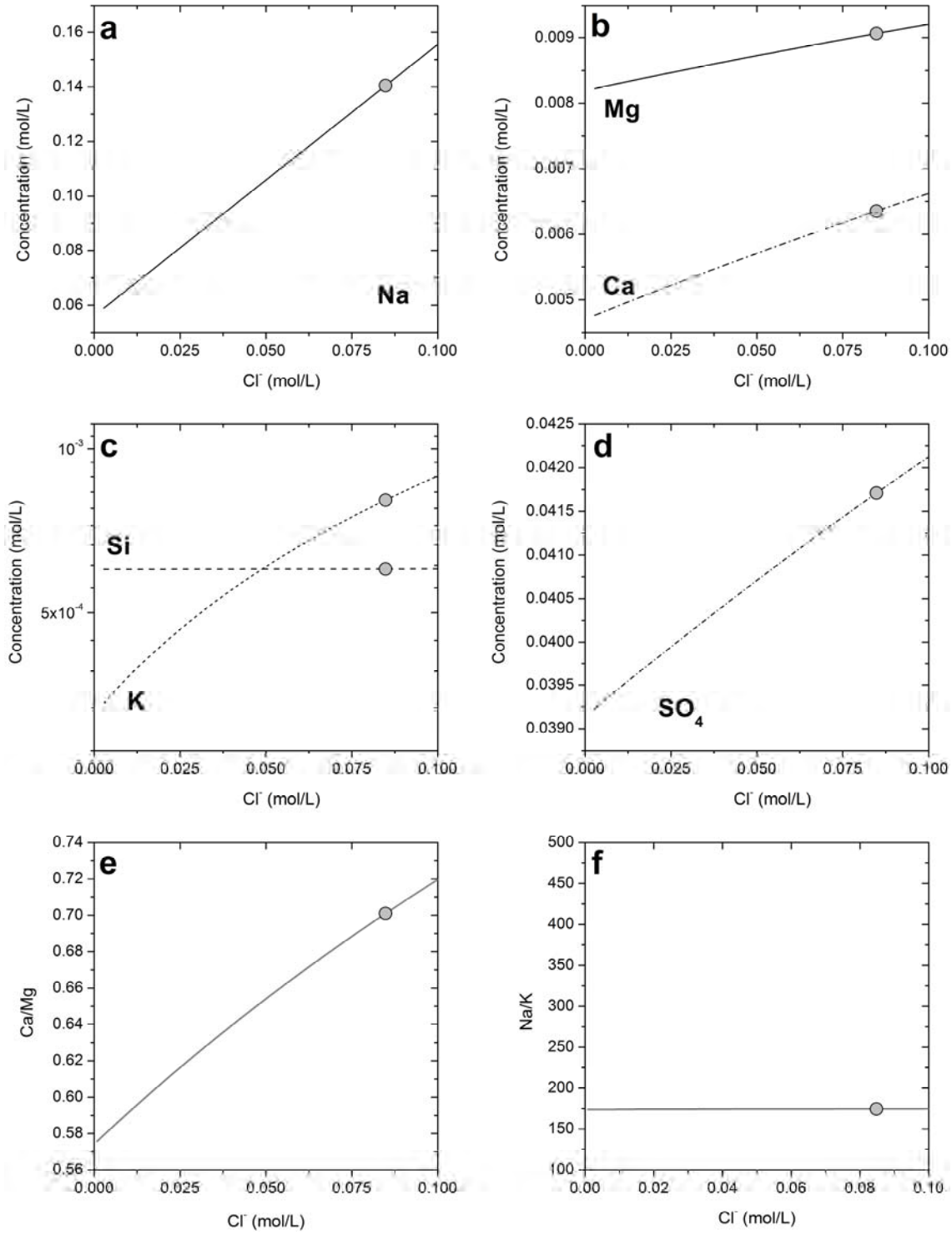

1045

1046 Figure 7

1047

1048

1049

Figure captions

Figure 1. Location of the Tiermas geothermal system and geological map of the area (modified from Oliva-Urcia *et al.*, 2012).

Figure 2. Cross section showing the general structure of the Jaca-Pamplona Basin and the location of Tiermas Springs (modified from ALGECO2 project: http://info.igme.es/algeco2/; IGME, 2010).

Figure 3. $\delta^2H - \delta^{18}O$ diagram showing the isotopic composition of sample T1, two samples from the Yesa Reservoir (one taken in 1985 and the other in 2012, this last one still unpublished) and one sample from a borehole in Tiermas from the study performed by Baeza *et al.* (2000). The Global Meteoric Water Line (GMWL), the Regional Meteoric Water Line (RMWL) and Local Meteoric Water Line (LMWL) are also represented.

Figure 4. Location of all the samples in the Giggenbach diagram. The dotted line is calculated with the Na-K Fournier (1979) calibration and with the Giggenbach (1988) one for Mg-K; the solid line is calculated with Na-K and Mg-K calibrations of Giggenbach (1988). If the dotted line is considered, the samples of the group 2 are close of being fully equilibrated.

Figure 5. Evolution with temperature of the saturation indices of the minerals supposed to be in equilibrium with the water of samples T1 (a) and B1 (b) in the reservoir. These results were obtained after the theoretical CO_2 addition to compensate the CO_2 outgassing during the ascent of the waters. The modelling for sample B1 (panel b) has been performed by equilibrating the water with quartz and K-feldspar and therefore, they are not shown in the plot. Dolomite-dis is disordered dolomite and Albite_low is low temperature albite.

Figure 6. Evolution with temperature of the saturation indices of the minerals supposed to be in equilibrium with the waters of sample T3 in the reservoir. In this case the modelling has been performed by equilibrating the water with K-feldspar and that is why it is not shown in the plot. These results were obtained after the theoretical CO_2 addition to compensate the CO_2 outgassing during the ascent of the waters. Dolomite-dis is disordered dolomite and Albite_low is low temperature albite.

Figure 7. Variation of the concentration of major elements (Na, Mg, Ca, Si, K and SO_4, panels a to d) and of the ratios Ca/Mg and Na/K (as total element concentrations; panels e and f) in sample T3 with the variation of the dissolved chloride in the waters at 82 ºC and maintaining the mineral equilibria that exist in the reservoir (albite, K-feldspar, quartz, anhydrite, calcite and dolomite). The grey dots in all the plots represent the chemical composition of sample T3.

1079